#6456

Energy and Buildings, *18* (1992) 65–75

Two-dimensional simulation of airflow and thermal comfort in a room with open-window and indoor cooling systems

J. Niu and J. van der Kooi

Laboratory for Refrigeration and Indoor Climate Technology, Delft University of Technology, Mekelweg 2, 2628 CD, Delft (Netherlands)

(Received September 8, 1991; accepted December 1, 1991; revised paper received February 4, 1992)

Abstract

This paper presents the two-dimensional numerical simulation results of the ventilation rates, indoor airflow fields and temperature distributions in an office room with open windows and auxiliary cooling devices. The standard k–ϵ turbulence model is used for flow pattern and temperature predictions. Possible comfort problems are analyzed in terms of the percentage of dissatisfied (PD) people due to draught, as well as vertical temperature difference. The simulation results show that open windows can give a high ventilation rate due to the stack effect alone, and that good thermal comfort can be achieved when the outdoor temperature is moderate. However, thermal comfort analysis in terms of vertical temperature stratification and the PD value shows that discomfort can arise due to draughts near the floor and the too-large vertical temperature gradient in the occupied zone when the outdoor temperature is too low, and that a cooling radiator located below the window presents the same problems. The results also indicate that a lightly cooled ceiling makes the air temperature more uniform in the room. It is also shown that both of the cooling systems, when combined with open windows, can have a good energy efficiency.

Keywords: numerical simulation, thermal comfort, open-window ventilation

1. Introduction

Since a large proportion of people in modern society spend most of their time indoors, the indoor air quality in residences, offices and other indoor non-industrial environments has been an issue of increasing concern [1]. Indoor pollutants are normally at higher concentrations than their outdoor counterparts. Therefore, ventilation is needed to remove the contaminants and odours from the indoor environments. On the other hand, ventilation may cost energy during heating or cooling seasons. The potential of energy saving in ventilation therefore comprises a reduction of the amount of ventilation air supplied and the adoption of the best strategy for supplying this quantity of air in order to achieve maximum ventilation performance in the occupied zone without the discomfort of draughts or the creation of zones where the minimum ventilation rate is not achieved. To realize this goal, one of the major design strategies that should be considered is to control the flow patterns of the supplied air [2]. For mechanical ventilation, for example, this can be done by appropriately locating the positions of the air supply and exhaust in a room [3–7].

In contrast, the airflow route in a room with natural ventilation is difficult to control since natural ventilation is subject to the vagaries of weather. Wind speed and direction, and the temperature difference will not only affect the rate of fresh air supply but will also determine whether any opening will act as an inlet or outlet for the air space, and hence the path the air takes within the building [7]. To reduce the variations due to weather, a possible way is to maximize the buoyancy effect and minimize the wind effect [8]. This can be done by maximizing the height between the purpose-provided openings. To ensure that the individual rooms have adequate ventilation, it is possible to provide dual upper and lower vent openings on the same floor. Such a window configuration is an important component in a passive indoor climate system developed by

0378-7788/92/$5.00

Paassen [9]. Year-round simulation by Lute and Paassen [10] has shown that reasonable indoor temperatures for thermal comfort can be maintained for the moderate Dutch climate with this system, but that mechanical cooling will be needed for a warmer climate, higher internal heat or light building structures.

However, for fully understanding the indoor thermal-comfort aspects of natural ventilation, as well as the possible energy savings in the seasons when the outdoor air can be used for free cooling, the airflow patterns and temperature distributions within the ventilated room need to be fully investigated. Also, combining indoor cooling systems such as cooling radiators with open-window ventilation to improve indoor thermal comfort needs estimation of the energy performances concerned. The most-widely-used one-point model for calculation of natural ventilation rate is obviously not adequate for these purposes. Further investigations may need full-scale *in situ* measurements of the detailed flow parameters. On the other hand, the development of computational fluid dynamics has enable us to perform 'numerical experiments' about airflow details [6, 11, 12]. Therefore, numerical simulations of several typical open-window situations were conducted prior to full-scale *in situ* measurements. In this paper, details of these preliminary simulations are reported.

2. Case set-up

The simulation research was conducted for an office room as illustrated in Fig. 1(a), 4.5 m long, 2.7 m high and 4 m wide. The facade has a glazing area of almost the whole width and a height of 1.5 m. The lower and upper part of the glazing can be opened separately, each with a maximum opening of 0.5 m in height. This configuration of the room is similar to the test cell reported in refs. 9 and 10. It is assumed that there are two office workers and two computer terminals present in the room. Taking into account lighting and solar radiation, the overall internal heat in the present situation is assumed to be 45 W/m^2 floor area. For simplicity, the whole situation is simplified into a two-dimensional issue, as illustrated in Fig. 1(b). The thermal effect of the occupants and electric appliances are lumped together and represented by a rectangular blockage, with 200 W convective heat. Since the 2-D simplification means that the width considered is one metre, the 200 W internal heat corresponds to 45 W/m^2 floor area.

Six different situations are simulated and analyzed. The differences between the cases are the outdoor temperatures, window openings and internal cooling systems. Case 1 to case 3 are intended to compare the differences at different outdoor temperatures. Case 4 to case 6 are intended to compare the performances of different indoor cooling devices at high outdoor temperatures. In case 4, a cooling radiator with a cooling capacity of 100 W is placed below the window. In case 5 and case 6, the ceiling is assumed to be cooled or partly cooled, with a cooling capacity of 80 W and 37 W respectively. The details are given in Table 1. In summary, these cases may represent a room with moderately high internal heat situated in a moderate climate, and the outdoor air temperatures considered are possible for free cooling.

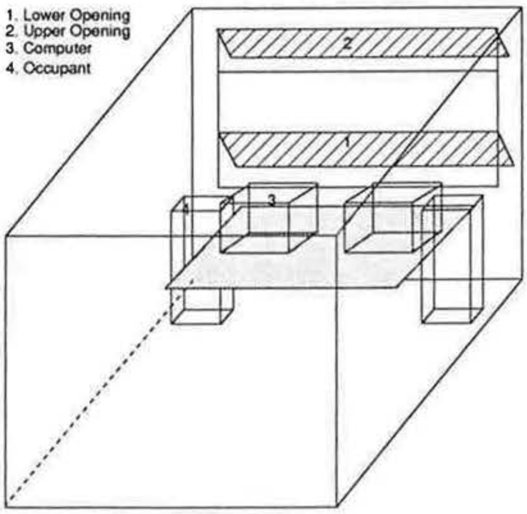

(a)

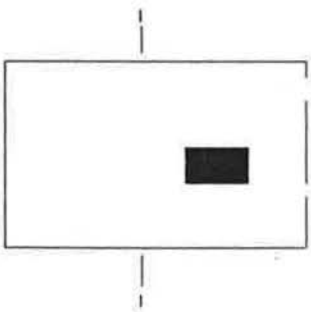

(b)

Fig. 1. Sketch of the simulation cases. (a) Configurations of the room. (b) 2-dimensional simplification.

TABLE 1. Summary of the simulation cases

Case no.	Case description	Opening size (m)		Temperatures (°C)		Simulation results	
		Upper	Lower	Outdoor	Wall	Ventilation rate (ach)	Ventilated heat (W)
1	Moderate outdoor temperature	0.5	0.5	20	22	13	200
2	Low outdoor temperature	0.05	0.03	15	22	4	170
3	High outdoor temperature	0.5	0.5	25	28	11	212
4	With a cooling radiator (100 W)	0.5	0.5	25	25	21	134
5	With a cooling ceiling (80 W)	0.5	0.5	25	25	23	120
6	With a partly cooled ceiling (37 W)	0.5	0.5	25	25	24	147

3. Mathematical formulation and method of solution

3.1. Airflow model

3.1.1. The turbulence model

Numerical simulation of the airflow and temperature distribution in the room involves the numerical solution of the mass conservation equation (continuity), momentum transport equations, and the energy transport equation [13]. One special difficulty of the solution of the equations comes from the fact that the flow encountered in rooms is turbulent, i.e., the velocity and temperature at a given point always fluctuate against time at rather high frequency [14, 15]. Therefore, certain turbulence models are developed for the purpose of the numerical solution. In recent years, they have been used for numerical prediction of airflows in rooms. Encouraging results, reviewed by Whittle (1986) and Nielson (1989), have been achieved. Among the models, the standard k–ϵ turbulence model [16] proves to be economically applicable and acceptable in prediction accuracy for engineering purposes. It should be mentioned that Tsutsumi [17] has used the large eddy simulation (LES) turbulence model to simulate the natural convection through window openings in a room. However, tremendous computer time and memories are needed for a simulation. In our study, the standard k–ϵ turbulence model is used.

In this model, two extra transport equations, in addition to the transport equations mentioned above, the turbulent kinetic energy (k) equation and the turbulence energy dissipation rate (ϵ) equation will also be solved. These equations are:

$$\frac{\partial u_i}{\partial x_i}=0 \tag{1}$$

$$u_j\frac{\partial u_i}{\partial x_j}=-\frac{1}{\rho}\frac{\partial p}{\partial x_i}+\frac{\partial}{\partial x_j}\left[(\nu_t+\nu_l)\frac{\partial u_i}{\partial x_j}\right]+\beta(T_0-T)g_i \tag{2}$$

$$u_j\frac{\partial H}{\partial x_j}=\frac{\partial}{\partial x_j}\left[\left(\frac{\nu_t}{\sigma_H}+\frac{\lambda}{\rho C_p}\right)\frac{\partial H}{\partial x_j}\right] \tag{3}$$

$$u_j\frac{\partial k}{\partial x_j}=\frac{\partial}{\partial x_j}\left[\left(\frac{\nu_t}{\sigma_k}+\nu_l\right)\frac{\partial k}{\partial x_j}\right]+\nu_t\left(\frac{\partial u_i}{\partial x_j}+\frac{\partial u_j}{\partial x_i}\right)\times\frac{\partial u_i}{\partial x_j}-\epsilon+\beta\frac{\nu_t}{\sigma_H}\frac{\partial(T-T_0)}{\partial x_i}g_i \tag{4}$$

$$u_j\frac{\partial \epsilon}{\partial x_j}=\frac{\partial}{\partial x_j}\left[\left(\frac{\nu_t}{\sigma_2}+\nu_l\right)\frac{\partial \epsilon}{\partial x_j}\right]+C_1\nu_t\frac{\epsilon}{k}\times\left(\frac{\partial u_i}{\partial x_j}+\frac{\partial u_j}{\partial x_i}\right)\times\frac{\partial u_i}{\partial x_j}-C_2\frac{\epsilon^2}{k}+C_3\frac{\epsilon}{k}\beta\frac{\nu_t}{\sigma_H}\frac{\partial(T-T_0)}{\partial x_j}g_j \tag{5}$$

where the turbulent viscosity is given by:

$$\nu_t=C_\mu k^2/\epsilon \tag{6}$$

where the empirical constants are: $\sigma_k=1.0$, $\sigma_\epsilon=1.3$, $\sigma_H=0.9$, $C_1=1.44$, $C_2=1.92$, $C_3=1.44$ and $C_\mu=0.09$.

With the standard k–ϵ turbulence model, special boundary conditions have to be specified to take into account the friction effect and heat transfer from a solid wall. In the program PHOENICS, the logarithmic wall function is used [16]. It must be noted that the convection heat transfer thus calculated will depend on the distance of the first grid-node from the wall, and therefore, the first grid-node distance from the wall needs to be optimized. According to Renz *et al.* [18], the friction and heat transfer from the wall thus predicted are in good agreement with measurements. For convective heat from the internal heat source, fixed flux boundary conditions are set for the adjacent air. It is assumed that 80 W are convected into the air from the top and 60 W from each of the two vertical sides of the block.

3.1.2. Model of the openings

The calculations are restricted to the domain inside the room. The influence of the outdoor conditions on the indoor climate is represented by an appropriate boundary condition at the openings. In the present simulations, only the influence of the indoor and outdoor temperature difference is investigated, therefore the boundary condition will reflect this nature. It must be noted that, in the momentum equation (eqn. (2)), the pressure p only stands for the relative pressure due to the nature of velocity variation, and that the gravity effect is combined in the buoyancy term $\beta(T_0 - T)g_i$ in the same equation [19]. Therefore, the outside pressures near the two openings are assumed to be the same and equal to the atmospheric pressure $P_0 = 0$, i.e., the variation of the absolute static pressure due to gravity at the different height is (and must be) omitted for the boundary conditions at the openings. Furthermore, in the lower opening, where inflow is expected, the stagnation pressure of the computation grid-nodes there is assumed to be equal to the atmospheric pressure, i.e.,

$$\frac{\rho v_i^2}{2} + P_i = P_0 \tag{7}$$

and the temperature of the inflow air is outdoor temperature; while the static pressure at the higher opening, where outflow is expected, is assumed to be equal to the atmospheric pressure P_0. This boundary specification is based on the Bernoulli equation, and friction at the openings is neglected. Details about how this is done in the numerical schemes can be found in ref. 20.

3.2. Numerical schemes and algorithms for solution

The governing differential equations are discretized by finite-volume method; upward differencing is used to reflect the physical nature that convection is an asymmetric phenomenon [13, 21]. The staggered grids are used to locate the discretized grid-nodes for velocity components, enthalpy and pressures, which is known as the SIMPLE procedure. In PHOENICS, the SIMPLE method is enhanced and an extra equation is solved for the evolution of pressure [22].

3.3. Model for the analysis of thermal comfort in rooms

Thermal comfort is defined as "that condition of mind in which satisfaction is expressed with the thermal environment". Therefore, both thermal environment and personal variables influence thermal response and comfort. In modern offices, the occupants tend to be in a moderate activity level. It was found that persons with lower activity levels are sensitive to draughts [23], an undesired local cooling of the human body caused by air movement [24, 25].

Fanger *et al.* [26] developed a mathematical model to quantify the draught risk in terms of the percentage of dissatisfied people. In this model, the percentage dissatisfied people due to draughts, PD(%), is calculated from

$$\mathrm{PD} = (34 - T_a)(V - 0.05)^{0.62}(3.14 + 0.37VI) \tag{8}$$

for $V < 0.05$ m/s insert $V = 0.05$ m/s, and for PD > 100 let PD = 100, where T_a is the local air temperature (°C), V is the mean velocity (m/s), and I is the turbulence intensity (%), which is defined as the velocity fluctuation over the mean velocity. The turbulent intensity can be calculated from

$$I = 100(2k)^{0.5}/V \tag{9}$$

The values of T_a, V and k can be obtained from the airflow calculation, and therefore, the PD distribution can be calculated.

In most cases in buildings, the air temperature normally increases with height above the floor. If the gradient is sufficiently large, local warm discomfort can occur at the head and/or cold discomfort can occur at the feet, although the body as a whole is thermally 'neutral'. The few experimental investigations that have been conducted to examine the influence of the vertical temperature difference on human comfort are reviewed in the ASHRAE handbook [27]. It was found that people are more sensitive to the positive temperature difference — higher above and lower below — and less sensitive to the negative vertical temperature differences. In the research conducted by Olesen *et al.* [28], seated subjects in their preferred average temperatures were subjected to vertical temperature differences of different magnitude. It was found that when the temperature difference is larger than 3 °C between head (1.1 m above the floor) and ankles (0.1 m above the floor), the percentage of dissatisfied people increases drastically. In the ISO standard [29], it is recommended that this vertical temperature difference be less than 3 °C.

In the present study, eqn. (9) will be used to evaluate the draught risks in the open-window situations investigated. Since the PD index does not take into account the influence of the temperature stratification, the overall thermal comfort will also be analysed from the temperature stratifications.

4. Results and discussions

The simulated ventilation rates and the heat carried away by the ventilated air of the six cases are listed in Table 1. The temperature stratifications of all the cases are illustrated in Fig. 2, in which the temperatures in the section I–I indicated in Fig. 1 are plotted against the height. The graphical forms of velocity vectors, isotherms (contours of temperature), turbulent kinetic energies and the percentage of dissatisfied people due to draught are illustrated in Figs. 3–8.

Case 1

Case 1 is to simulate the situation when the outdoor temperature is moderate. The outdoor air temperature is assumed to be 20 °C. In reality, most people would open their windows to welcome this mild, fresh air. Correspondingly, the simulated results are also promising. With the two windows fully open, a ventilation rate as high as 13 ach is achieved. The average air temperature in the occupied zone is approximately 21 °C (Fig. 3(c)), while the temperature difference between the heights 0.1 m and 1.1 m is less than 0.5 °C, as illustrated in Fig. 2. In the occupied zone, the air velocities are lower than 0.1 m/s (Fig. 3(a)), and the turbulent kinetic energy (k) is lower than 10^{-4} J/kg (Fig. 3(b)). The draught risk, calculated from eqn. (9) is illustrated in Fig. 3(d), which shows that, in most of the region in the room, the PD value is nearly zero. It indicates that there is little risk of draught.

Looking at the flow patterns illustrated in Fig. 3(a), it is clear that the thermal plume formed around the internal heat source plays a dominant role. The entrainment of the thermal plume produces the recirculation flows in the upper space of the room. Similar to the flows in a displacement ventilation situation [3], the recirculation flows appear above a certain height, at which the entrained flow rate is equal to the supplied flow rate from below, and this height depends on the supplied flow rate. In this case, it can be seen from Fig. 3(a) that part of the fresh air is entrained into the hot plume directly, while the other part tends to flow downward. The overall flow pattern is thus formed.

Case 2

Now that it has been shown that open-window ventilation has a positive effect in every aspect concerned with comfort when the outdoor temperature is moderate, Case 2 is to simulate the situation of opening the windows at a relatively lower outdoor temperature, at 15 °C in this case. The lower and upper openings are assumed to be 30 mm and 50 mm wide slots, respectively.

A ventilation rate of 4 ach is obtained, at which the average air temperature in the occupied zone ranges from 20 to 24 °C, as illustrated in Fig. 4(c). The temperature difference between the height 0.1 m and 1.1 m is as large as 3.2 °C, which is greater than the recommended value 3 °C [29]. The air velocity near the lower opening is about 0.3 m/s (Fig. 4(a)), and the generated turbulence is much higher than in case 1. The maximum value of k is about 2×10^{-3} J/kg (Fig. 4(b)). Consequently, it can be seen from Fig. 4(d) that the local PD due to draught near the floor is rather high, which indicates that occupants may feel too cold at their ankles and/or knees.

The flow pattern illustrated in Fig. 4(a) shows that the fresh air comes downward towards the floor

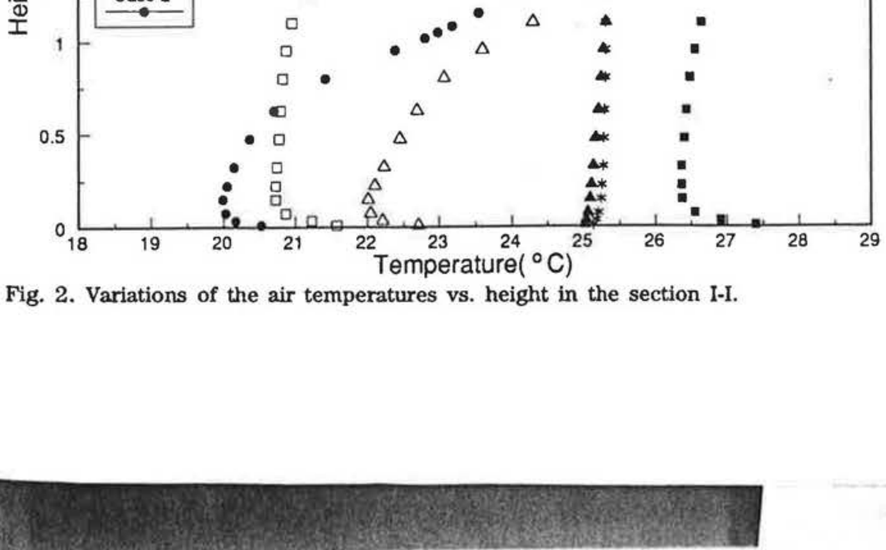

Fig. 2. Variations of the air temperatures vs. height in the section I-I.

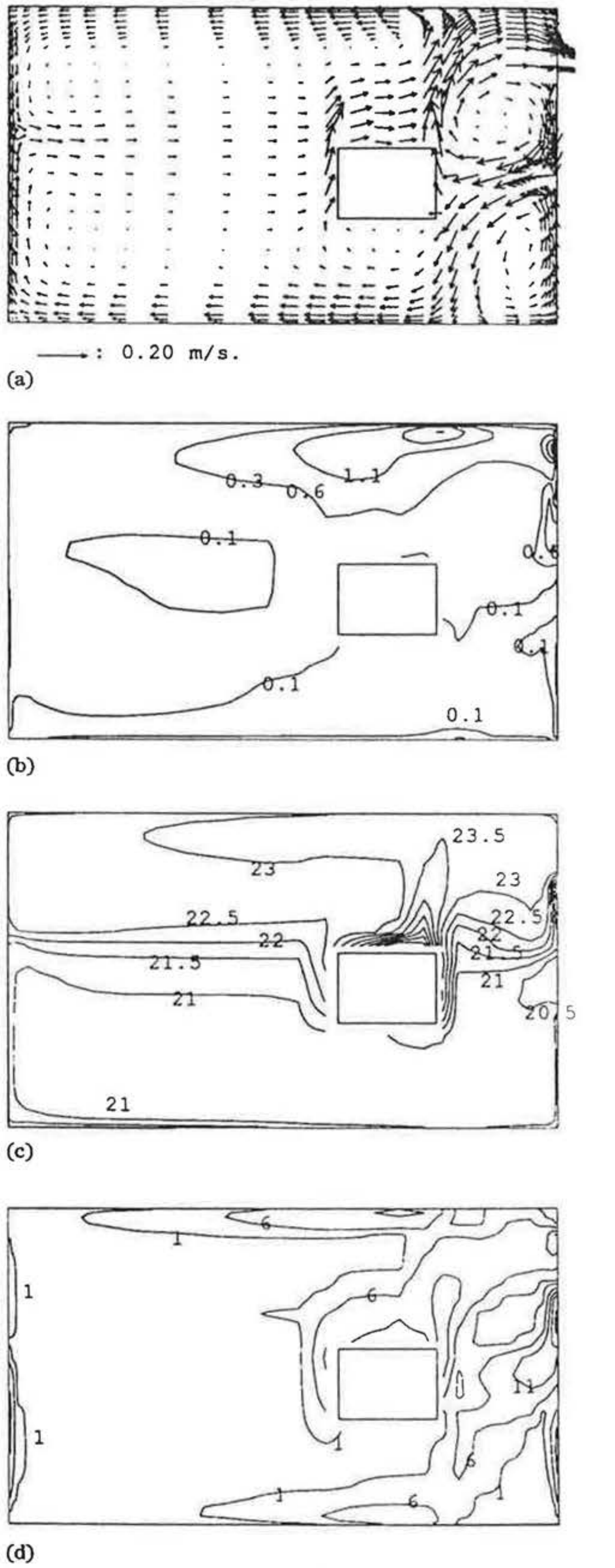

Fig. 3. Simulated field distributions of case 1. (a) Velocity vectors. (b) Contours of $k(10^{-3}$ J/kg). (c) Isotherms (°C). (d) Percentage dissatisfied people (%) due to draught.

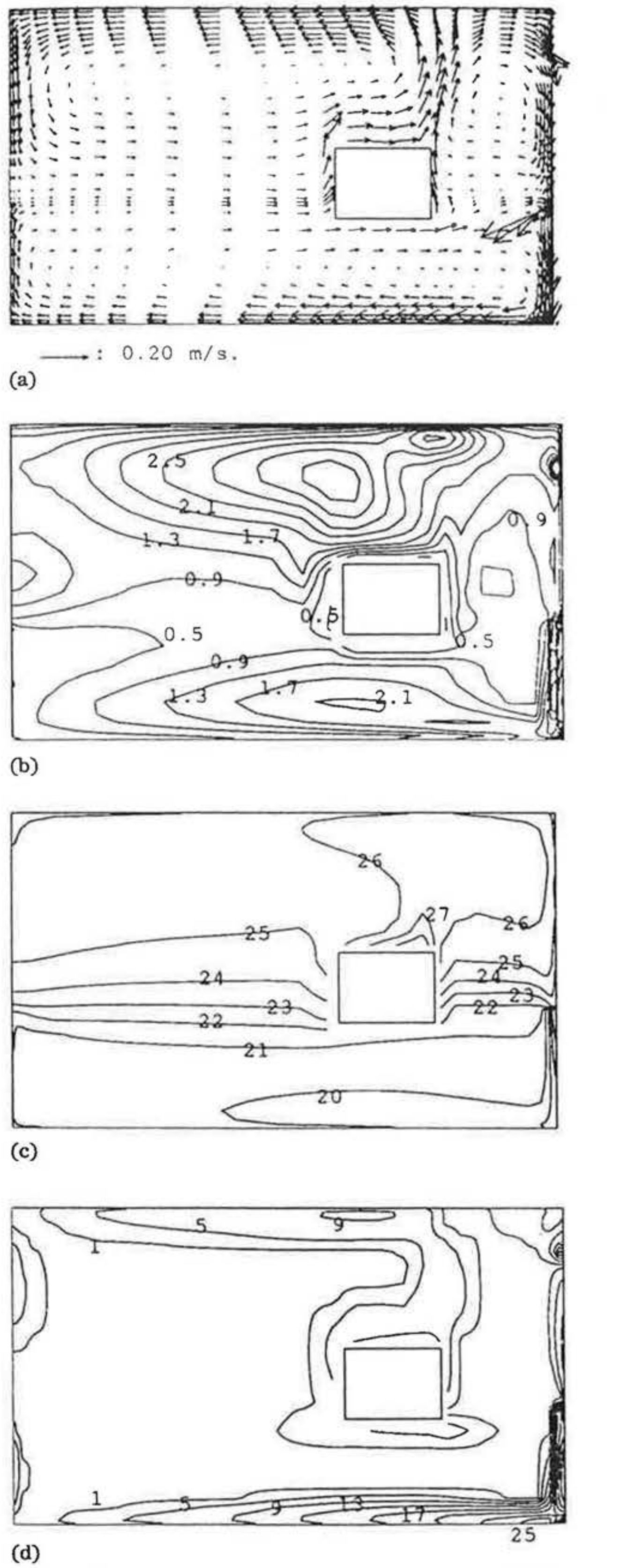

Fig. 4. Simulated field distributions of case 2. (a) Velocity vectors. (b) Contours of $k(10^{-3}$ J/kg). (c) Isotherms (°C). (d) Percentage dissatisfied people (%) due to draught.

immediately after admitted, because of its low temperature. This phenomenon is rather different from that in case 1 (Fig. 3(a)). It is because of this characteristic of the flow that the temperature stratification is more severe, and worse from the point of view of thermal comfort. To avoid this, one possibility is to raise the temperature of the outdoor air in one way or another before it is admitted into the occupied space and also to increase the airflow rate. This may indicate that the minimum temperature of the outdoor air that can be used for free cooling simply through natural ventilation is limited by, among other things, thermal comfort requirements.

Case 3

This case simulates a 'summer' situation: the outdoor air temperature is 25 °C and the internal wall surface temperature is assumed to be 28 °C. Compared with case 1, the indoor–outdoor temperature difference is 3 K instead of 2 K, while all the other conditions are the same. Therefore, the simulated flow pattern, turbulent kinetic energy distribution (Fig. 5(a) and (b)), as well as the temperature stratification (Fig. 2) are similar to those in case 1, and only the average temperature level is higher. The ventilation rate is 11 ach, and the average air temperature in the occupied zone is about 26.5 °C. The temperature difference between the heights 0.1 m and 1.1 m is less than 0.5 °C. Since the air temperature is rather high, the PD due to draught is very low.

However, it is possible that it is too warm in the room if the radiant environment is taken into account. Therefore, the following simulation cases, cases 4–6, are set up to investigate the possibilities of auxiliary indoor cooling combined with open-window ventilation.

Case 4

A convective cooling radiator with a cooling capacity of 100 W is placed below the window. The radiant effect of the radiator is taken into consideration by setting the wall internal surface temperature to 25 °C.

The flow pattern is rather different in this case (Fig. 6(a)). A short-circuit occurs for the ventilated flow. Almost all the fresh air is entrained into the hot plume directly, and then circulated to the upper opening immediately. Due to this short-circuit effect, the ventilation rate is rather high — 21 ach, and 134 W of heat, nearly 70% of the total internal heat, are carried away by ventilation.

The lower zone of the room is dominated by the recirculation flow caused by the cooling radiator

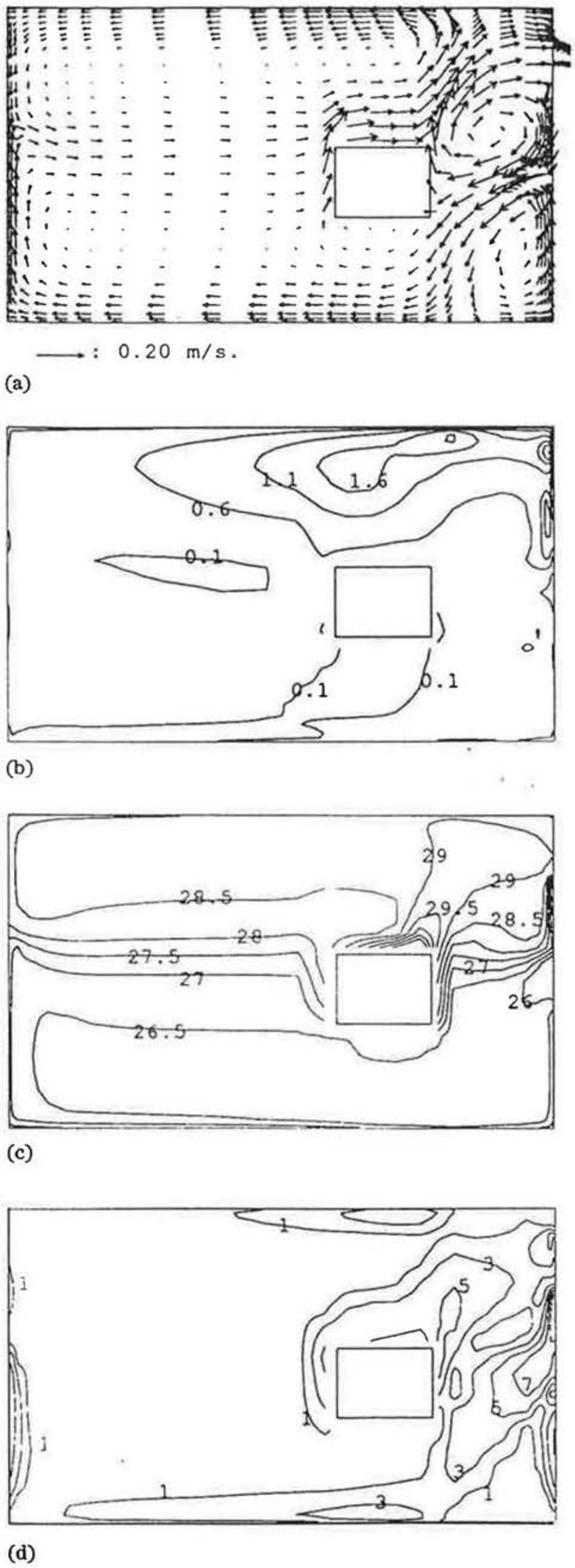

Fig. 5. Simulated field distributions of case 3. (a) Velocity vectors. (b) Contours of $k(10^{-3}$ J/kg). (c) Isotherms (°C). (d) Percentage dissatisfied people (%) due to draught.

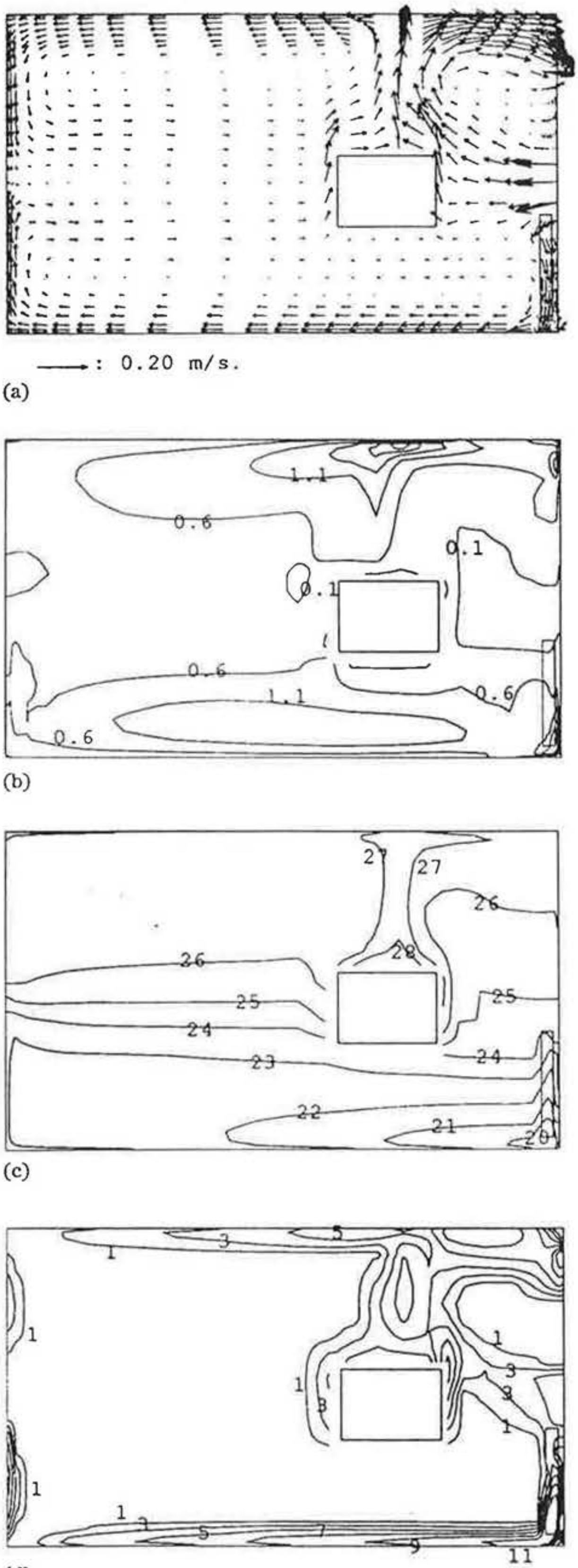

Fig. 6. Simulated field distributions of case 4. (a) Velocity vectors. (b) Contour of $k(10^{-3}$ J/kg). (c) Isotherms (°C). (d) Percentage dissatisfied people (%) due to draught.

and is not much affected by the ventilation air. Due to the buoyancy effect, the cooled air from the cooling radiator tends to flow in such a way that it sticks to the floor. As a result, rather severe temperature stratification exists: the temperature difference between the heights 0.1 m and 1.1 m is nearly 2.5 °C (Fig. 2). Though this value is lower than 3 °C, this stratification will be enhanced by the radiant effect of the radiator [27, 30]. Therefore, a cooling radiator located below the window may not be ideal for thermal comfort. It should be noted that the turbulent kinetic energy near the floor is around 0.6×10^{-3} J/kg (Fig. 6(b)), which, according to eqn. (9), will contribute to the discomfort due to draught. On the other hand, the cooling energy from the cooling radiator is well preserved in the lower part of the room, and the ventilation does not cause much loss of this energy. Therefore, the energy efficiency can be satisfactorily high.

Case 5

As an alternative, the whole ceiling is assumed to be 'lightly' cooled with a convective cooling capacity of approximately 18 W/m^2, which is equivalent to the assumption that the temperature difference is about 5 °C and the convective heat transfer coefficient $\alpha_c = 4$ W/m^2 K. As in case 4, the radiant effect is taken into account by setting the wall surface temperature to 25 °C.

The simulated flow pattern is illustrated in Fig. 7(a). As can be seen, two main recirculation streams are formed: one is the cooled downward stream along the rear wall from the ceiling, which is subsequently entrained by the thermal plume; the other one is the ventilated air stream. The consequent temperature distribution is rather uniform and the temperature ranges between 25 °C and 25.5 °C in the occupied zone (Fig. 7(c)). The temperature stratification is small. Therefore, the temperature distribution is ideal for thermal comfort. However, the turbulent kinetic energy is rather high, ranging from 0.1×10^{-3} to 2.1×10^{-3} J/kg in the occupied zone (Fig. 7(b)). The PD due to draught is slightly high along the rear wall (Fig. 7(d)). This may suggest that the ceiling should be lightly cooled to avoid strong downward convective flows.

Still, a high ventilation rate can be maintained, and the ventilation air carries away 60% of the internal heat. There is a fear that opening the window while the ceiling is cooled may lose energy. In the present simulation, this does not occur since there is always a thermal plume in the room. However, it can be seen that the thermal plume is slightly cooled by the ceiling before being discharged (Fig. 7(c)). If the internal heat source is located further

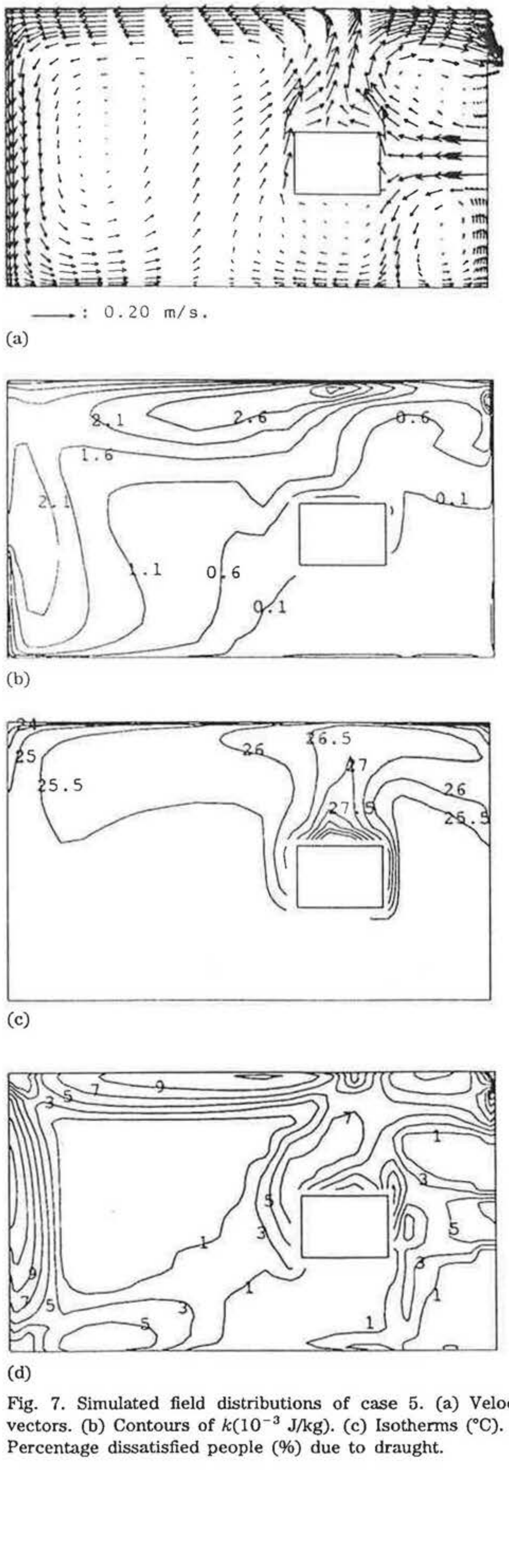

Fig. 7. Simulated field distributions of case 5. (a) Velocity vectors. (b) Contours of $k(10^{-3}$ J/kg). (c) Isotherms (°C). (d) Percentage dissatisfied people (%) due to draught.

away from the window, the discharged air would be further cooled. This cooling of the exhaust air is obviously a waste of energy.

Case 6

Different from case 5, only the inner half of the ceiling is assumed to be cooled, with a cooling capacity of approximate 16 W/m^2 (37 W in total). With this small cooling, the temperatures (Fig. 8(c)) can still be much lower in comparison with case 3. The flow patterns, turbulent kinetic energy (Fig. 8(a) and (b)) are about the same as in case 5. The PD due to the draught from the ceiling is much reduced (Fig. 8(d)). The temperature stratification is small (Fig. 2). Most significant is that the cooling energy needed is much reduced, since nearly 75% of the internal heat is carried away by the ventilation air.

5. Concluding remarks

For the room with a moderately high internal heat, the lower and upper dual-window configuration can give a high ventilation rate due to the buoyancy effect alone. At moderate outdoor temperatures, the resulting temperature distribution in the room is good for thermal comfort. However, at relatively low outdoor temperatures, the resulting vertical temperature difference can be too large for thermal comfort, though the average temperature within the room is moderate. Therefore, the comfort requirement may limit the minimum temperatures at which free cooling by natural ventilation through the dual window openings can function well. When indoor cooling devices are combined with the dual window openings, it is shown that the positions of the cooling surfaces are important both for thermal comfort and for energy efficiency. A cooling radiator situated below the window tends to give a large vertical temperature difference in the occupied zone, which is not desirable for thermal comfort. When the ceiling is lightly cooled, the resulting temperature distribution in the whole room becomes rather uniform. As far as energy efficiency is concerned, both of the cooling systems can be fairly good as long as the outdoor temperature is not too high.

6. Further studies

The results of the preliminary two-dimensional simulation highlight the possibility of maximizing the buoyancy effect by providing dual window openings. It may indicate that, even during windless

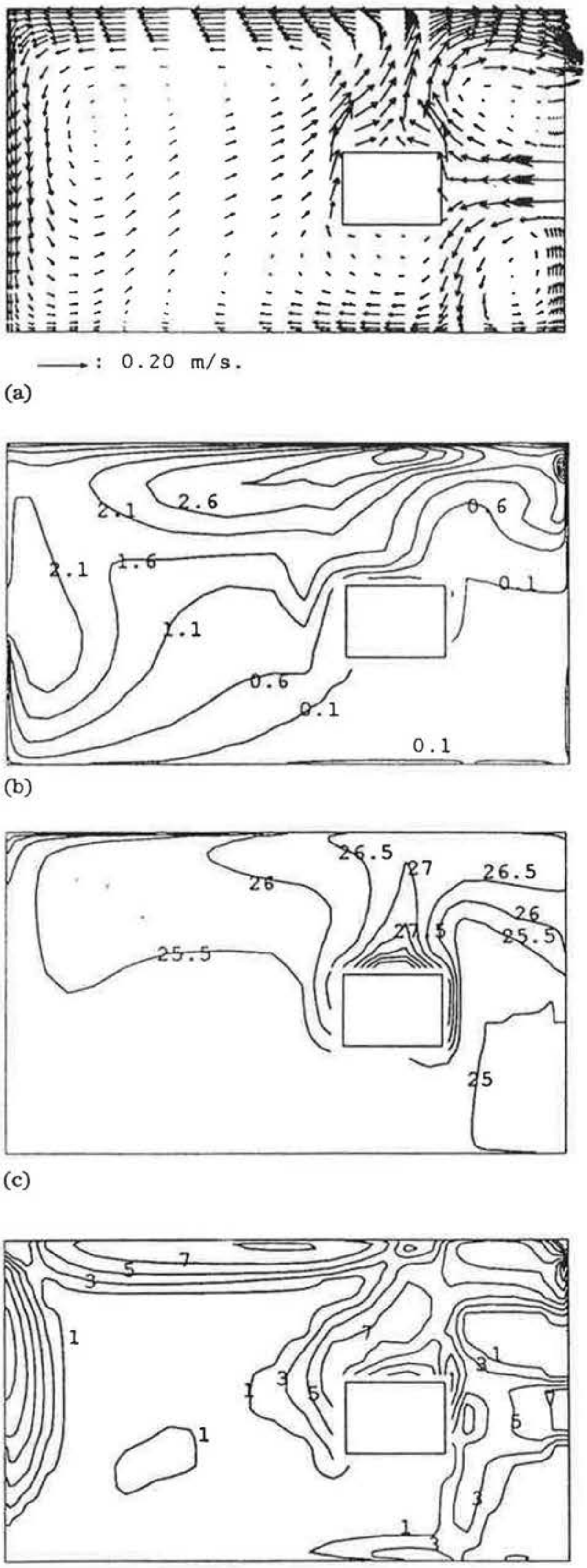

Fig. 8. Simulated field distributions of case 6. (a) Velocity vectors. (b) Contours of $k(10^{-3}$ J/kg). (c) Isotherms (°C). (d) Percentage dissatisfied people (%) due to draught.

days, a high ventilation rate can be achieved through such a window. Though it can be expected that wind will generally increase the natural ventilation rate, what influence wind will have on the ventilation through the dual window openings will be a point of further investigations.

Nomenclature

ach	air exchange rate per hour in a ventilated room, defined as the ventilated airflow rate divided by the room volume (1/hour)
C_p	specific heat of air (J/kg)
C_μ, C_1, C_2, C_3	empirical constants in the k–ϵ turbulence model
g_i	gravitational acceleration components in ith direction (m/s^2)
H	enthalpy (J/kg)
I	turbulent intensity (%)
k	turbulent kinetic energy (J/kg)
p	relative pressure of air (Pa)
PD	percentage dissatisfied people (%)
P_i	relative pressure at the inlet opening (Pa)
P_0	relative atmospheric pressure (Pa)
T	temperature of air (K)
T_a	air temperature (°C)
T_0	reference temperature (K)
u_i, u_j	velocity components in ith and jth directions (m/s)
V	mean velocity of air (m/s)
ν_i	velocity at the inlet opening (m/s)
x_i, x_j	Cartesian coordinates (m)
β	thermal expansion coefficient of air 1/K)
ϵ	dissipation rate of turbulence energy (W/kg)
λ	thermal conductivity of air (W/m K)
ν_l	laminar viscosity of air (m^2/s)
ν_t	turbulent viscosity of airflow (m^2/s)
ρ	density of the air (kg/m^3)
σ_H	turbulent Prandtl number
σ_k	turbulent Schmidt number of k
σ_ϵ	turbulent Schmidt number of ϵ

References

1 Air contaminants, *ASHRAE Handbook – 1985 Fundamentals*, Ch. 11, p. 11.9.

2 G. W. Brudrett, Requirements for ventilation, *Proc. CIBS Symposium Natural Ventilation by Design, London, Dec. 1980*, p. 1–7.

3 P. Kofoed and P. V. Nielson, Thermal plumes in ventilated rooms – An experimental research work, *Proc. 3rd Seminar on Application of Fluid Mechanics in Environmental Protection 1988*, Silesian Technical University, Gliwice, Poland.

4 E. Skaret and H. Mathisen, Ventilation efficiency, *Proc. Int. Symposium on Indoor Pollution, Health and Energy Conservation*, Massachusetts, MA, October 13–16, 1981.

5 M. Sandberg, Definition of ventilation efficiency and the efficiency of mechanical ventilation systems, *Proc. 3rd AIC Conf. Energy Efficient Domestic Ventilation Systems for Achieving Acceptable Indoor Air Quality*, September 20–23, 1982, UK, pp. 13.1–13.22.

6 Q. Chen, J. van der Kooi and A. Meyers, Measurements and computations of ventilation efficiency and temperature efficiency in a ventilated room, *Energy Build.*, *12* (1988) 85–99.

7 J. E. Holt, Problems in commercial and industrial ventilation, *Proc. CIBS Symposium Natural Ventilation by Design, Dec., 1980, London*, pp. 35–44.

8 D. Etherridge, Domestic ventilation system design – changes in the wind? *Watson House Bull.*, *46* (3) (1982) 12–16.

9 A. H. C. van Paassen, Passive solar energy in intelligent buildings, *ASHRAE Trans.*, *94* (1) (1988) 1289–1297.

10 P. J. Lute and A. H. C. van Paassen, Integrated control system for low energy buildings, *Proc. ASHRAE Symposium Building Operation Dynamics, Louis, Missouri, June 9–13, 1990.*

11 P. V. Nielson, Progress and trends in air infiltration and ventilation research, *Proc. 10th AIVC Conf., Coventry*, Air Infiltration and Ventilation Centre, Warwick, UK, 1989.

12 Q. Chen, C. A. Meyers and J. van der Kooi, Convective heat transfer in rooms with mixed convection, *Proc. Int. Seminar on Air Flow Patterns in Ventilated Spaces, Liège*, The National Fund of Scientific Research in Belgium, pp. 69–82.

13 S. V. Patankar, Convection and diffusion, *Numerical Heat Transfer and Fluid Flow*, McGraw-Hill, 1980, Ch. 5.

14 A. Melikov, H. Hanzawa and P. O. Fanger, Airflow characteristics in the occupied zone of heated spaces without mechanical ventilation, *ASHRAE Trans.*, *94* (1988) 52–70.

15 H. Hanzawa, A. Melikov and P. O. Fanger, Airflow characteristics in the occupied zone of ventilated spaces, *ASHRAE Trans.*, *93* (1987) 524–539.

16 B. E. Launder and D. B. Spalding, The numerical computation of turbulent flow, *Comp. Methods Appl. Mech. Eng.*, *3* (1974) 269–289.

17 J. Tsutsumi, Numerical simulation of thermal convection in a room with natural ventilation caused by buoyancy, *Proc. CIB W67 Symposium on Energy Moisture and Climate in Buildings, Rotterdam, Netherlands, Sept., 1990.*

18 U. Renz and U. Terhaag, Predictions of air flow pattern in a room ventilated by an air jet – the effect of turbulence model and wall function formulation, *Proc. ROOMVENT'90, Engineering Aero- and Thermodynamics of Ventilated Room: 2nd Int. Conf., Oslo, Norway, June 13–15, 1990.*

19 D. J. Tritton, Convection, *Physical Fluid Dynamics*, Clarendon, Oxford, 1988, 2nd edn., Ch. 14, pp. 163–165.

20 H. I. Rosten and D. B. Spalding, *The PHOENICS Reference Manual*, CHAM TR/200, Oct., 1987, Ch. 6, pp. 6.91–6.92.

21 S. V. Patankar, Recent developments in computational heat transfer, *Trans. ASME – J. Heat Transfer*, *110* (1988) 1037–1045.

22 H. I. Rosten and D. B. Spalding, How PHOENICS operates, *The Phoenics Beginner's Guide*, CHAM TR/100, Oct., 1987, Ch. 2, pp. 2.10–2.15.

23 B. W. Jones, K. Hsieh and M. Hashinaga, The effect of air velocity on the thermal comfort at moderate activity levels, *ASHRAE Trans.*, *92* (Part 2B) (1986) 761–769.

24 P. O. Fanger and N. Christensen, Perception of draught in ventilated spaces, *Ergonomics*, *29* (2) (1986) 215–235.

25 D. A. McIntyre, The effect of air movement on thermal comfort and sensation, in P. O. Fanger and O. Valbjorn (eds.), *Indoor Climate*, Danish Building Research Institute, Copenhagen, 1979, pp. 541–560.

26 P. O. Fanger, A. Melikov, H. Hanzawa and J. Ring, Air turbulence and sensation of draught, *Energy Build.*, *12* (1988) 21–39.

27 Physiological principles, comfort, and health, *ASHRAE Handbook – 1989 Fundamentals*, Ch. 8, pp. 8.20–8.22.

28 B. W. Olesen, M. Scholer and P. O. Fanger, Vertical air temperature differences and comfort, in P. O. Fanger and O. Valbjorn (eds.), *Indoor Climate*, Danish Building Research Institute, Copenhagen, 1979, pp. 561–579.

29 *International Standard ISO 7730, Moderate thermal environments – Determination of the PMV and PPD indices and Specification of the conditions for thermal comfort*, Ref. No. 7730–1984(E), August, 1984, p. 5.

30 Radiant heating and cooling, *ASHRAE Handbook – 1991 HVAC Applications*, SI edition, Ch. 48, pp. 48.4–48.5.